World Journal of Gastrointestinal Oncology

Submit a Manuscript: https://www.f6publishing.com

World J Gastrointest Oncol 2025 April 15; 17(4): 103843

DOI: 10.4251/wjgo.v17.i4.103843

ISSN 1948-5204 (online)

ORIGINAL ARTICLE

Basic Study

Nitric oxide synthase 1 inhibits the progression of esophageal cancer through interacting with nitric oxide synthase 1 adaptor protein

Zi-Wei Xiao, Ying-Chao Zeng, Lin-Tao Ji, Jia-Tao Yuan, Lin Li

Specialty type: Oncology

Provenance and peer review: Unsolicited article; Externally peer reviewed.

Peer-review model: Single-blind

Peer-review report's classification

Scientific Quality: Grade B, Grade C

Novelty: Grade B, Grade B

Creativity or Innovation: Grade B, Grade C

Scientific Significance: Grade B, Grade C

P-Reviewer: Wang YJ; Yu Y

Received: December 3, 2024

Revised: January 22, 2025

Accepted: February 17, 2025

Published online: April 15, 2025

Processing time: 113 Days and 9.1 Hours

Zi-Wei Xiao, Ying-Chao Zeng, Lin-Tao Ji, Jia-Tao Yuan, Lin Li, College of Medical, Hunan Normal University, Changsha 410081, Hunan Province, China

Corresponding author: Lin Li, Associate Professor, College of Medical, Hunan Normal University, No. 36 Lushan Road, Changsha 410081, Hunan Province, China. 18529482372@163.com

Abstract

BACKGROUND

Esophageal cancer (ESCA) is among the most prevalent and lethal tumors globally. While nitric oxide synthase 1 (NOS1) is recognized for its important involvement in various cancers, its specific function in ESCA remains unclear.

AIM

To explore the potential role and underlying mechanisms of NOS1 in ESCA.

METHODS

Survival rates were analyzed using GeneCards and Gene Expression Profiling Interactive Analysis. The effects and mechanisms of NOS1 on ESCA cells were evaluated *via* the Cell Counting Kit-8 assay, scratch assay, Transwell assay, flow cytometry, quantitative polymerase chain reaction, western blotting, and terminal deoxynucleotidyl transferase-mediated deoxyuridine triphosphate-biotin nick end labeling staining. The protein interaction network was used to screen the interacting proteins of NOS1 and validate these interactions through co-immunoprecipitation and dual luciferase assays. Additionally, a nude mouse xenograft model was established to evaluate the effect of NOS1 *in vivo*.

RESULTS

The survival rate of patients with ESCA with high NOS1 expression was higher than that of patients with low NOS1 expression. NOS1 expression in ESCA cell lines was lower than that in normal esophageal epithelial cells. Overexpression of NOS1 (oe-NOS1) inhibited proliferation, invasion, and migration abilities in ESCA cell lines, resulting in decreased autophagy levels and increased apoptosis, pyroptosis, and ferroptosis. Protein interaction studies confirmed the interaction between NOS1 and NOS1 adaptor protein (NOS1AP). Following oe-NOS1 and the silencing of NOS1AP, levels of P62 and microtubule-associated protein 1 light

chain 3 beta increased both *in vitro* and *in vivo*. Furthermore, the expression levels of E-cadherin, along with the activation of phosphatidylinositol 3-kinase (PI3K) and protein kinase B (AKT), were inhibited in ESCA cell lines.

CONCLUSION
NOS1 and NOS1 proteins interact to suppress autophagy, activate the PI3K/AKT pathway, and exert anti-cancer effects in ESCA.

Key Words: Nitric oxide synthase 1; Nitric oxide synthase 1 adaptor protein; Autophagy; Phosphatidylinositol 3-kinase/protein kinase B pathway; Esophageal cancer

Core Tip: Nitric oxide synthase 1 (NOS1) inhibits the proliferation, metastasis, apoptosis, pyroptosis, and ferroptosis of esophageal cancer (ESCA) cells; enhances the autophagy; and effectively delays the onset of ESCA in a nude mouse xenograft model. Mechanistically, NOS1 interacts with the NOS1 adaptor protein, inhibiting the activation of the phosphatidylinositol 3-kinase/protein kinase B pathway. Both *in vitro* and *in vivo* studies suggest that NOS1 is a potential therapeutic target for ESCA.

Citation: Xiao ZW, Zeng YC, Ji LT, Yuan JT, Li L. Nitric oxide synthase 1 inhibits the progression of esophageal cancer through interacting with nitric oxide synthase 1 adaptor protein. *World J Gastrointest Oncol* 2025; 17(4): 103843
URL: https://www.wjgnet.com/1948-5204/full/v17/i4/103843.htm
DOI: https://dx.doi.org/10.4251/wjgo.v17.i4.103843

INTRODUCTION

Esophageal cancer (ESCA) is an exceptionally aggressive disease with a notably poor prognosis[1]. Diagnosis generally occurs at a later stage when metastatic spread has already taken place, since individuals with ESCA often lack clinical symptoms in the early phases, and the cancer usually proliferates quickly[2]. Various forms of cell death, including apoptosis, autophagy, necrosis, pyroptosis, and ferroptosis, significantly influence the survival of ESCA cells. Importantly, autophagy within cells is linked to both pro-tumor and anti-tumor reactions in relation to ESCA[3-6]. Studies have shown that disruptions in mitochondrial bioproduction can lead to mitochondrial DNA stress, triggering the cyclic guanosine monophosphate-adenosine monophosphate synthase-stimulator of interferon genes pathway and stimulating autophagy, which subsequently aids the advancement of esophageal squamous cell carcinoma[7]. Research indicates that the BTN3A1 protein can trigger autophagy by enhancing *ULK1* activity in esophageal squamous cell carcinoma cells[8]. Additionally, the activation of autophagy contributes to the development of resistance against various treatments across different tumor types. In ESCA, autophagy serves a protective function, enabling tumor cells to withstand the damages caused by radiotherapy and contributing to chemotherapy *via* signaling pathways such as epithelial-mesenchymal transition, phosphatidylinositol 3-kinase/protein kinase B (PI3K/AKT), and other mechanisms[9,10].

Cellular autophagy serves as a protective mechanism for cells and is vital in sustaining intracellular balance within normal human cells. Different kinds of cellular stresses trigger autophagy, which helps break down cellular components and supports cell survival[11,12]. Conversely, cancerous tumor cells can take advantage of autophagy, using it as a shield to survive in the harsh conditions of the tumor microenvironment[13]. Autophagy can promote cancer growth and spread through various pathways, while also increasing the resistance of tumor cells to treatments, primarily owing to its protective abilities during cancer progression[14,15]. Furthermore, nitric oxide (NO) is crucial in modulating autophagy; for example, NO suppresses autophagy in cardiomyocytes by activating guanylate cyclase[16]. In the context of hepatocellular carcinoma, NO hinders autophagy by interfering with the interaction between Beclin 1 and vacuolar protein sorting 34, while also encouraging apoptosis through the increased attachment of *Bcl-2* to Beclin 1[17].

NO, produced by NO synthases (NOS), can also be formed non-enzymatically through the nitrate-nitrite-NO pathway. This molecule acts as a powerful cellular messenger integral to the intricate processes regulating autophagy, serving as a negative modulator of this mechanism[18]. Moreover, NO is acknowledged as a crucial factor in both carcinogenesis and tumor development, influencing a range of cancer-related activities. The NOS1 isoform, alongside NO, is associated with tumor growth, including processes such as angiogenesis, apoptosis, invasion, and metastasis[19,20]. The gene for the NO synthase 1 adaptor protein (NOS1AP) encodes a protein that associates with the NOS1 enzyme, interacts with its binding sites, and alters the activity of NOS1[21]. This research aims to explore the role of NOS1 in the development of ESCA and analyze how NOS1AP expression affects NOS1 function, cellular autophagy, and the production of NO, ultimately offering new perspectives on the treatment of ESCA.

MATERIALS AND METHODS

Cell and reagents

Het-1A, KYSE-70, TE-9, TE-15, and OE-19 cells were purchased from the American Type Culture Collection (Manassas, USA). Microtubule-associated protein 1 light chain 3 beta (LC3B) antibody (14600-1-AP), and P62 antibody (18420-1-AP) were purchased from Proteintech (Wuhan, China). Beclin 1 antibody (ab207612), *ULK1* antibody (ab229909), *Bax* antibody (ab289364), *Bcl-2* antibody (ab182858), pro-Caspase-1 antibody (ab179515), ASC antibody (ab309497), caspase 3 antibody (ab184787), cleaved-Caspase 3 antibody (ab32042), *GPX4* antibody (ab125066), *SLC7A11* antibody (ab307601), glyceraldehyde-3-phosphate dehydrogenase antibody (ab8245), and goat anti-rabbit IgG H + L [horseradish peroxidase (HRP)] (b6721) were purchased from Abcam (Cambridge, UK). Goat anti-mouse IgG/HRP (SE131) was purchased from Solarbio (Beijing, China). *Fth1* antibody (P02794) was purchased from Abmart (Shanghai, China). Cleaved-Caspase-1 antibody (YBC0002) was purchased from YBio (Shanghai, China).

Bioinformatics analysis

The GeneCards database (https://www.genecards.org/) was used to explore the functions associated with the *NOS1* gene. The Gene Expression Profiling Interactive Analysis (GEPIA) tool (http://gepia.cancer-pku.cn/index.html) was employed to assess the expression levels of the *NOS1* gene in ESCA and adjacent non-cancerous tissues. Subsequently, survival curves were generated based on the expression of the *NOS1* gene in these contexts, utilizing the log-rank test and the Mantel-Cox test for statistical evaluation. Additionally, the NOS1 protein interaction network was examined using the STRING database (http://string-db.org), and the GEPIA database was further used to investigate the correlation between the identified proteins and NOS1.

Quantitative polymerase chain reaction

Total RNA was extracted using the Tiangen Universal Reagent (DP424, Tiangen, Beijing, China) and subsequently analyzed using a one-step quantitative real-time polymerase chain reaction kit (B639277, Sangon, Shanghai, China) to measure the expression of *Bcl-2*, *Bax*, Caspase 3, p-p38, and p-p65. All protocols were conducted following the manufacturer's instructions. The mRNA expression levels were normalized to the internal reference gene β-actin and calculated using the $2^{-\Delta\Delta Ct}$ method.

Western blotting

Proteins were extracted utilizing radioimmunoprecipitation assay lysis buffer lysate, according to the manufacturer's instructions. Protein separation was performed through sodium dodecyl sulfate-polyacrylamide gel electrophoresis, followed by transfer onto polyvinylidene fluoride membranes, which were then blocked with a 5% skimmed milk powder solution. The primary antibody was applied to the membrane and incubated overnight at 4 °C. After washing with phosphate-buffered saline (PBS), the membranes were incubated for 2 h with the secondary antibody at room temperature. Protein bands were visualized using the enhanced chemiluminescence detection reagent (P0018S, Beyotime, Shanghai, China).

Cell transfection

The overexpression of NOS1 (oe-NOS1), silencing of NOS1AP, and related negative controls were synthesized by Tsingke Biotech Co., Ltd. (Beijing, China). Following the manufacturer's guidelines, Lipofectamine 3000 (Invitrogen, Carlsbad, USA) was employed to transfer small interfering RNAs, overexpression RNAs, and empty vectors into the cells. The efficacy of the infection was confirmed using quantitative polymerase chain reaction and western blotting (WB).

Cell function assay

For the invasion assay, cells were seeded into Transwell upper chambers coated with Matrigel. Complete medium was added to the corresponding lower well plates. After 24 hours, the medium from the lower chambers was discarded, and the cells were fixed with 4% paraformaldehyde for 20 min. After washing with PBS, crystal violet solution was applied and incubated for 30 min. After three additional PBS washes, the chambers were filled with PBS for subsequent microscopic observation. For the scratch assay, cells were cultured in a dish and allowed to grow for 24 h. A vertical scratch was created using a pipette tip, after which the medium was replaced with a fresh complete medium. The width between scratches in each group was measured after 24 h to assess cell migration. For the cell counting kit-8 (CCK-8) assay, cells were plated in a 96-well plate. Diluted cell counting kit-8 reagent was added to each well to assess proliferative capacity, incubated for 10 minutes in the dark, and the optical density of each well was measured using a spectrophotometer.

TUNEL staining

The cell culture medium was discarded, and the cells were gently rinsed with PBS before being fixed with 4% paraformaldehyde for 30 min. After removal of the fixative, the cells were gently washed, and equilibration buffer was applied dropwise for 10 min. Subsequently, terminal deoxynucleotidyl transferase incubation buffer was applied dropwise, and the samples were incubated in the dark. Thereafter, 4',6-diamidino-2-phenylindole staining was conducted for 3 min. The cells were washed with PBS, fresh PBS was added to each well, and the samples were examined under a microscope. Sections were exposed to varying concentrations of xylene and ethanol solutions for dewaxing and rehydration. After rinsing with double distilled water, proteinase K was applied for DNA repair, and endogenous peroxidase activity was

inhibited using 3% hydrogen peroxide (H_2O_2). The sections were then incubated in an HRP-conjugated working solution at 37 °C, and color development was achieved using the diaminobenzidine method. The sections were counterstained with hematoxylin, differentiated with 1% hydrochloric acid alcohol to decolorize the background, rinsed with double-distilled water, and air-dried.

Flow analysis

A cell cycle assay was conducted using the DNA content assay kit (Cell Cycle) (CA1510, Solarbio, Beijing, China). Digested cells were rinsed with PBS and gradually treated with 5 mL of pre-cooled 70%-80% ethanol. They were then incubated overnight at 4 °C in the dark. After ethanol removal, the cells were resuspended in an appropriate volume of PBS, followed by the addition of propidium iodide dye and RNase. The mixture was incubated for 15 min in the dark before analysis using a BD fluorescence-activated cell sorting Calibur flow cytometer. Apoptosis was detected using an Annexin V-fluorescein isothiocyanate/propidium iodide apoptosis detection kit (CA1040, Solarbio, Beijing, China).

Establishment of nude mouse xenograft model

Nude mice were obtained from the Guangdong Medical Laboratory Animal Center and kept in a standardized facility. The study was approved by the Animal Ethics Committee of Guangzhou Myers Biotechnology Co. (No. MIS20230070). A total of 5×10^6 cells in 100 μL were subcutaneously injected into 4-week-old nude mice. Body weight and tumor volume were measured every 7 days. At the end of the experimental period, the mice were euthanized, and the tumor tissues were excised for weight and volume measurements.

Hematoxylin staining

Tumor tissues were paraffin-embedded and prepared as pathological sections. Hematoxylin staining solution was applied dropwise to the tissue sections and they were incubated for 5 min, followed by rinsing with distilled water. The sections were then immersed in a bluing solution for 1 min, rinsed again with distilled water, and treated with eosin for 1 min. After another rinse with distilled water, the sections were sequentially immersed in ethanol solutions with concentrations of 75%, 85%, 95%, and 100% for 2-3 s each. Finally, the sections were dehydrated with anhydrous ethanol for 1 min, cleared with xylene twice for 1 min each, and sealed with tree resin.

Immunohistochemistry analysis

The sections were submerged in 10 mmol/L sodium citrate buffer at 95 °C for 20 min, then removed and treated dropwise with a 3% H_2O_2 solution for 10 min. After three washes with PBS, diluted antibodies were added, and the sections were incubated at 4 °C overnight. Following another three PBS washes, HRP-conjugated antibodies were applied and incubated for 2 h. After three more PBS washes, color development was achieved using diaminobenzidine.

Co-immunoprecipitation

Cells were collected and lysed in immunoprecipitation lysis buffer enriched with phenyl methane sulfonyl fluoride, and all procedures were conducted on ice. The resulting supernatant was incubated overnight at 4 °C with an antibody or IgG (AC005, ABclonal, Wuhan, China). The immunoprecipitated beads were subsequently washed three times, eluted with 1× protein sample buffer, and heated at 99 °C for 5 min. Following bead removal, WB was performed on the samples.

Dual luciferase assay

A reporter gene plasmid was constructed by inserting sequences from the *NOS1AP* gene, the firefly luciferase gene, and the sea kidney luciferase gene into the pGL3-basic vector. The plasmids were subsequently transfected into HEK293T cells using Lipofectamine 3000 and cultured for 48 h. After cultivation, cells were lysed following the instructions of the dual-luciferase reporter gene assay kit (RG088S, Beyotime, Shanghai, China), and fluorescence intensity was measured using a fluorometer.

Statistical analysis

Data were analyzed using GraphPad Prism 9.5.1, unless stated otherwise. Differences between two groups were analyzed using a one-way analysis of variance, with $P < 0.05$ deemed statistically significant.

RESULTS

NOS1 is downregulated in ESCA tissues

Table 1 illustrates the molecular functions of the *NOS1* gene, as detailed by Gene Ontology. This gene is linked to the modulation of NOS activity, oxidoreductase functions, as well as the activity of calcium and natriuretic ion channels. Additionally, it facilitates the interaction of various substrates, including arginine, metal ions, hemoglobin, transmembrane transporters, and scaffolding proteins, at their specific binding sites. The GEPIA database indicated that the expression of NOS1 in ESCA tumor tissues is lower than in normal tissues (Figures 1A and 1B). Kaplan-Meier survival analysis revealed that patients diagnosed with ESCA exhibiting elevated NOS1 expression demonstrated improved survival rates compared to those with lower expression levels (Figure 1C).

Table 1 Molecular functions of *NOS1* gene

GO ID	Qualified GO term	Evidence
0004517	Nitric-oxide synthase activity	IDA, ISS, IBA, TAS
0005246	Calcium channel regulator activity	TAS
0005515	Protein binding	IPI
0005516	Calmodulin binding	IEA
0010181	Flavin mononucleotide binding	ISS, IBA
0016491	Oxidoreductase activity	IEA
0017080	Sodium channel regulator activity	ISS
0020037	Heme binding	ISS
0034617	Tetrahydrobiopterin binding	NAS
0034618	Arginine binding	TAS
0044325	Transmembrane transporter binding	ISS, TAS
0046870	Cadmium ion binding	ISS
0046872	Metal ion binding	IEA
0048306	Calcium-dependent protein binding	ISS
0050660	Flavin adenine dinucleotide binding	ISS, IBA
0050661	NADP binding	ISS
0097110	Scaffold protein binding	ISS

GO: Gene ontology; IDA: Inferred from direct assay; ISS: Inferred from sequence or structural; IBA: Inferred from biological aspect of ancestor; TAS: Traceable author statement; IPI: Inferred from physical interaction; IEA: Inferred from electronic annotation; NAS: Non-traceable author statement.

NOS1 overexpression inhibits ESCA cell function

Expression levels of NOS1 were evaluated in human normal esophageal epithelial cells Het-1A and ESCA cell lines (KYSE-70, TE-9, TE-15, OE-19) utilizing quantitative polymerase chain reaction and WB, as shown in Figures 2A and 2B. NOS1 expression in the ESCA cell lines KYSE-70, TE-9, TE-15, and OE-19 was lower than that observed in Het-1A cells. Following this, further studies were performed to clarify the function of NOS1 within ESCA cells. TE-15 and OE-19, which exhibited the lowest NOS1 levels, were selected for detailed examination. Additionally, cell lines TE-15oe-NOS1 and OE-19oe-NOS1 were created to overexpress NOS1. Functional assays indicated that oe-NOS1 led to decreased proliferation, invasion, and migration alongside enhanced apoptosis in TE-15 and OE-19 cells (Figures 2C-2F and Supplementary Figure 1A). Flow cytometry analysis showed a gradual decline in the percentage of cells in the G2/M phase following the oe-NOS1 expression (Figure 2G and Supplementary Figure 1B).

NOS1 overexpression inhibits tumor growth in mice

Mice received subcutaneous injections of TE-15, OE-19, TE-15oe-NOS1, and OE-19oe-NOS1 cells to create tumor xenograft models, and the growth of the tumors was observed. The findings from immunohistochemical analysis indicated that the models created with NOS1-overexpressing cells displayed increased NOS1 expression within their tumor tissues (Figure 3A). Tumors formed from TE-15 and OE-19 cells overexpressing NOS1 appeared lighter and smaller (Figures 3B-3E). As a result, the weight loss in the mice was less pronounced (Figure 3F). Histopathological evaluation revealed that the tumor cells from the TE-15 and OE-19 groups were diverse, abundant, disordered, and exhibited intensely stained nuclei. In contrast, the NOS1-overexpressing groups, TE-15oe-NOS1 and OE-19oe-NOS1, showed a diminished cell count (Figure 3G).

NOS1 significantly affects autophagy levels in ESCA cells

WB revealed the expression levels of proteins linked to cellular mechanisms including autophagy, apoptosis, pyroptosis, and ferroptosis (Figure 4). Compared to TE-15 and OE-19 cells, the TE-15oe-NOS1 and OE-19oe-NOS1 cell lines showed a decreased expression of proteins including LC3II/LC3I, P62, Beclin 1, *ULK1*, *Bcl-2*, and *GPX4*. In contrast, there was an increase in the levels of *Bax*, cleaved-Caspase-3/Caspase-3, cleaved-Caspase-1/Caspase-1, cleaved-*GSDMD*/*GSDMD*, *ASC*, *Fth1*, and *SLC7A11*. The impact of NOS1 on the expression of autophagy-related proteins was notable. Analysis of protein interactions indicated that NOS1 might regulate the proteins involved in autophagy modulation (Figure 5), highlighting possible interactions with the *CALML* family (*CALM3*, *CALML1*, *CALML3*, *CALML4*, *CALML5*, *CALML6*), along with *GRIN2B*, *DI*, *RASD1*, and *SNTA1*. Moreover, correlation analysis pointed to a strong association between NOS1 and NOS1AP, while a weaker correlation was observed between NOS1 and *RASD1*, *CALM1*, *CALML3*, and

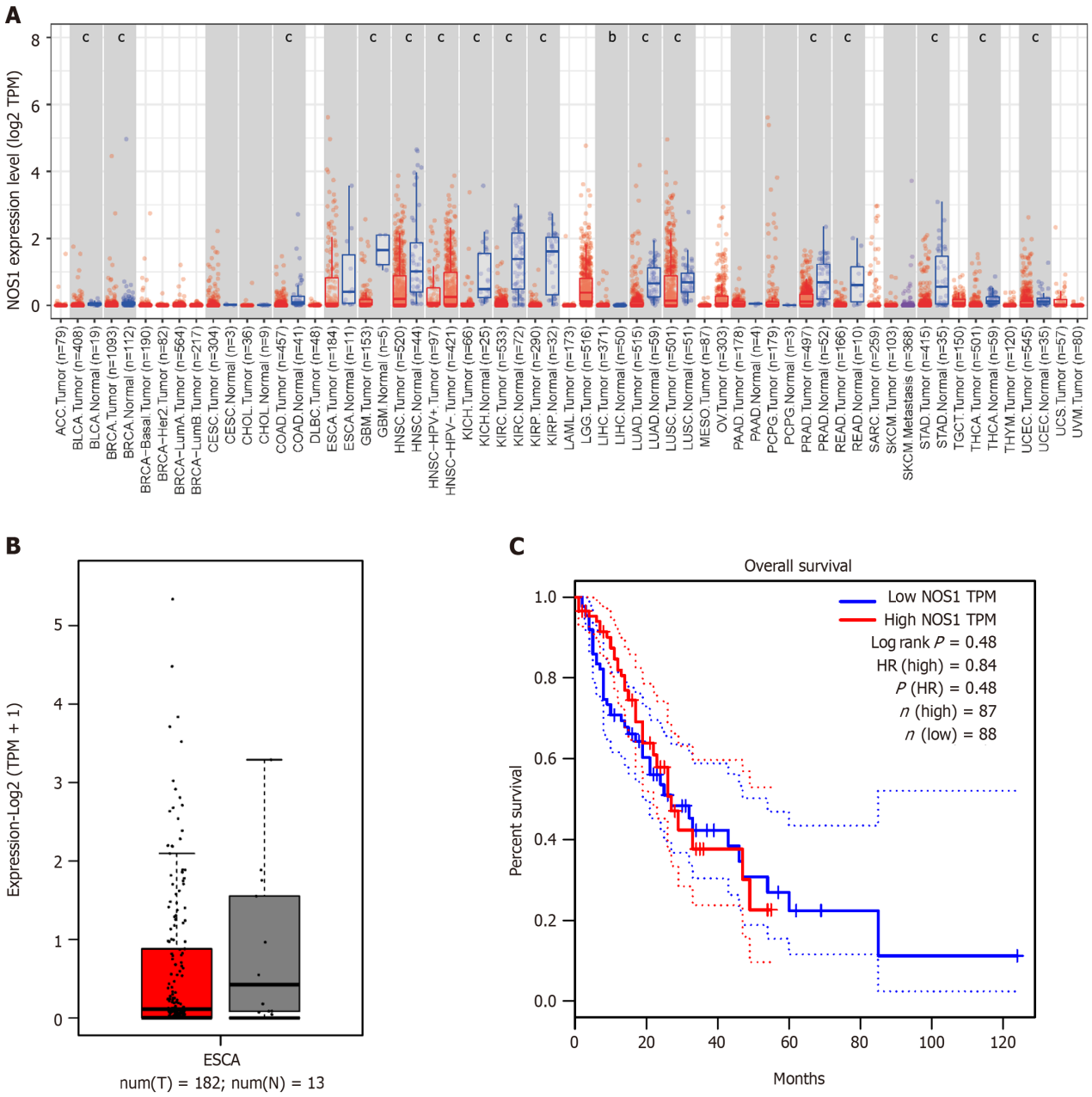

Figure 1 Expression of nitric oxide synthase 1 in different tissues and Kaplan-Meier analysis. A: Expression of nitric oxide synthase 1 (NOS1) in different tumor tissues and normal tissues; B: Expression of NOS1 in esophageal cancer tissues (left) and normal esophageal tissues (right); C: Relationship between the expression of NOS1 and overall survival of patients with esophageal cancer. $^{b}P < 0.01$. $^{c}P < 0.001$. ACC: Adrenocortical cancer; BLCA: Bladder cancer; BRCA: Breast cancer; CESC: Cervical cancer; CHOL: Bile duct cancer; COAD: Colon cancer; DLBC: Large B-cell lymphoma; ESCA: Esophageal cancer; GBM: Glioblastoma; HNSC: Head and neck cancer; HNSC-HPV: Head and neck cancer-human papillomavirus; KICH: Kidney chromophobe; KIRC: Kidney clear cell carcinoma; KIRP: Kidney papillary cell carcinoma; LAML: Acute myeloid leukemia; LGG: Lower grade glioma; LIHC: Liver cancer; LUAD: Lung adenocarcinoma; LUSC: Lung squamous cell carcinoma; MESO: Mesothelioma; OV: Ovarian cancer; PAAD: Pancreatic cancer; PCPG: Pheochromocytoma and paraganglioma; PRAD: Prostate cancer; READ: Rectal cancer; SARC: Sarcoma; SKCM: Melanoma; STAD: Stomach cancer; TGCT: Testicular cancer; THCA: Thyroid cancer; THYM: Thymoma; UCEC: Endometrioid cancer; UCS: Uterine carcinosarcoma; UVM: Ocular melanomas; TPM: Transcripts *per* million; NOS1: Nitric oxide synthase 1; HR: Hazard ratio.

CALML4 (Supplementary Figure 2).

NOS1 affects autophagy levels in ESCA cells in relation to NOS1AP expression levels

Co-immunoprecipitation analysis demonstrated that NOS1AP expression was observable *via* WB after immunoprecipitating using a NOS1 antibody (Figure 6A). In contrast, immunoprecipitation with an NOS1AP antibody allowed for the detection of NOS1 through WB, indicating a mutual interaction between the NOS1 and NOS1AP proteins. In the TE-15 or OE-19 cell lines, elevated levels of NOS1AP were observed as a result of NOS1 overexpression (Figures 6B and 6C). Additionally, the use of Autophagy-IN-5 to inhibit cellular autophagy resulted in elevated NOS1 and NOS1AP expressions in TE-15, OE-19, TE-15oe-NOS1, and OE-19oe-NOS1 cells (Figures 6D and 6E), along with a decrease in the levels of microtubule-associated protein 1 light chain 3-II/microtubule-associated protein 1 light chain 3-I (LC3II/LC3I)

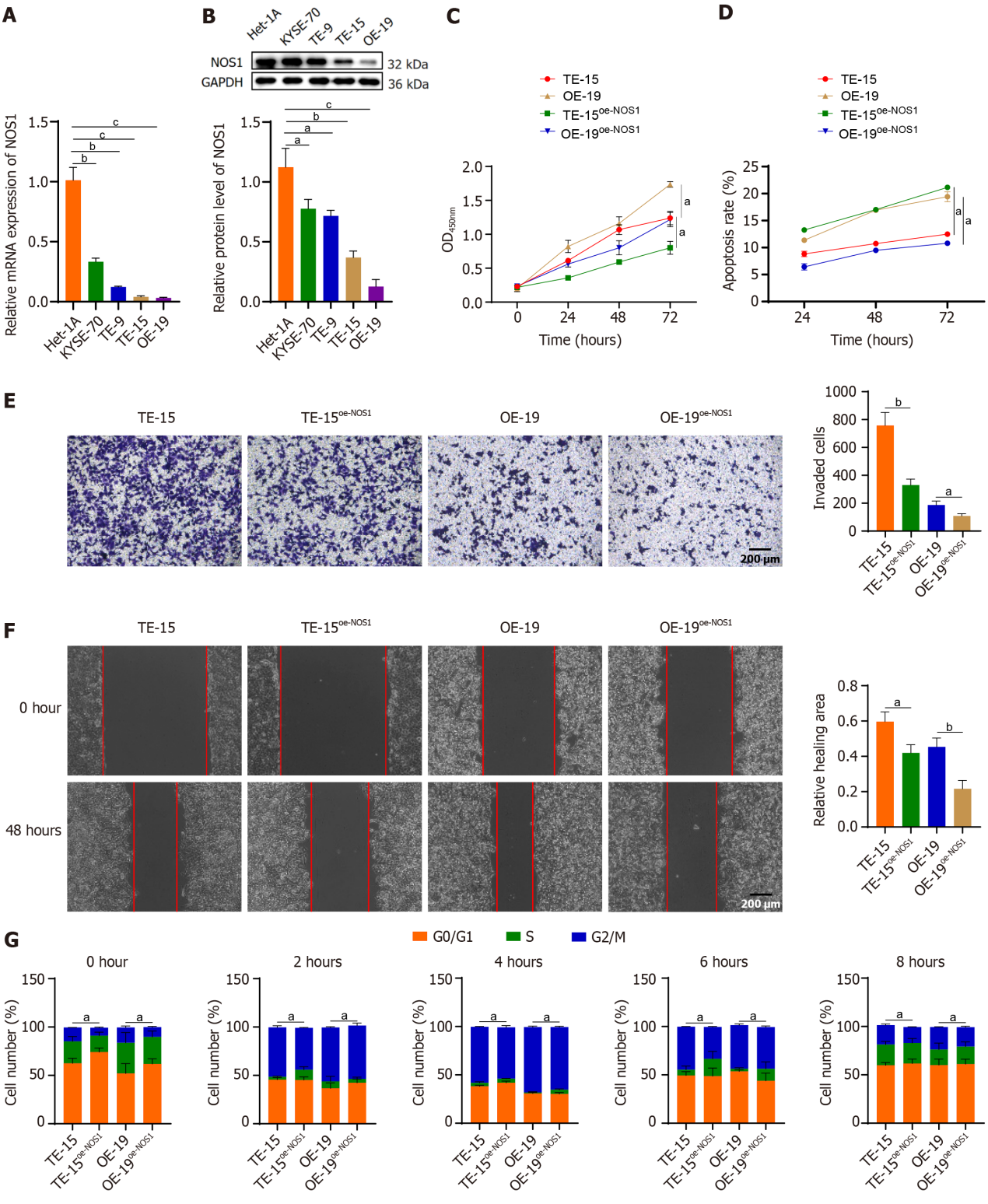

Figure 2 Effect of nitric oxide synthase 1 on esophageal cancer cell function. A: Quantitative real-time polymerase chain reaction to detect the expression of nitric oxide synthase 1 (NOS1) in Het-1A, KYSE-70, TE-9, TE-15, OE-19 cells; B: Western Blotting to detect the expression of NOS1 in Het-1A, KYSE-70, TE-9, TE-15, OE-19 cells.; C: Cell counting kit-8 to detect cell proliferation and viability; D: Flow cytometry to analyze the effect of NOS1 on cell apoptosis; E: Effect of NOS1 on cell invasion ability; F: Effect of NOS1 on cell migration ability; G: Effect of NOS1 on the cell cycle. Values are mean ± SD. $^{a}P < 0.05$. $^{b}P < 0.01$. $^{c}P < 0.001$. $n = 3$ experiments. NOS1: Nitric oxide synthase 1; oe-NOS1: Overexpression of nitric oxide synthase 1; OD: Optical density.

and P62 (Figures 7A and 7B), an increase in apoptosis (Figures 7C and 7D and Supplementary Figures 3A and 3B), and a reduction in proliferative capacity (Figure 7E and Supplementary Figure 3C). In scenarios of NOS1 overexpression combined with reduced levels of NOS1AP, the inhibition of autophagy led to increased levels of LC3II/LC3I and P62, diminished apoptosis, and improved proliferation. Immunohistochemical analysis indicated that the levels of LC3B and P62 in tumor tissues were reduced following NOS1 overexpression (Figures 7F and 7G). Additionally, P62 and LC3B expression levels were found to be elevated when NOS1 was overexpressed in combination with reduced levels of

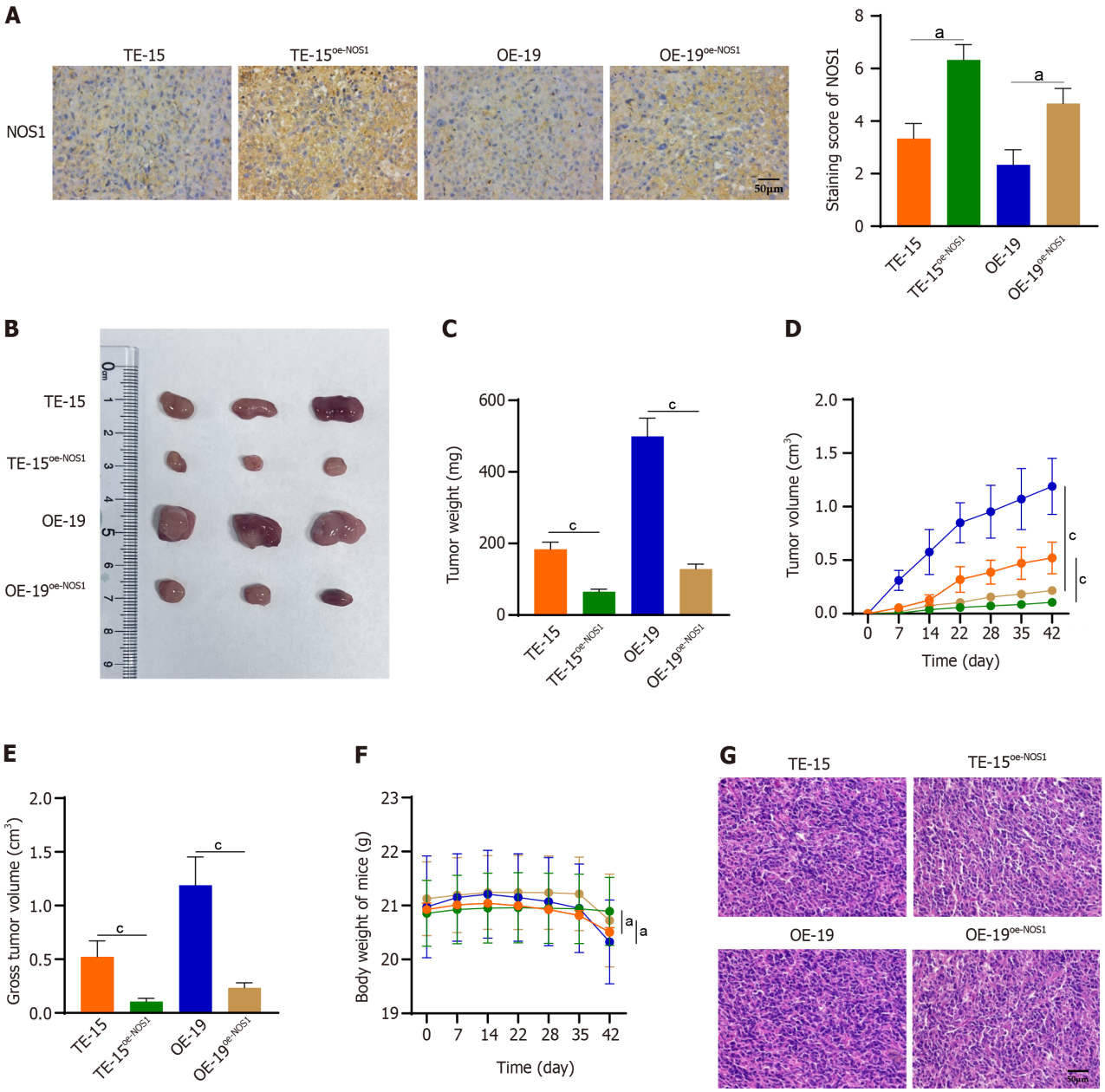

Figure 3 Effect of nitric oxide synthase 1 on tumor growth in mice. A: Expression of nitric oxide synthase 1 in tumor tissues detected by immunohistochemistry; B: Representative images of tumors; C: Tumor weight; D: Daily tumor volume; E: Total tumor volume; F: Body weight of mice; G: Tumor tissues stained with hematoxylin-eosin. Values are mean ± SD. $^{a}P < 0.05$. $^{b}P < 0.01$. $^{c}P < 0.001$. $n = 3$ experiments. NOS1: Nitric oxide synthase 1; oe-NOS1: Overexpression of nitric oxide synthase 1.

NOS1AP.

Expression of NOS1 and NOS1AP together affect the PI3K/AKT pathway

The expression levels of nitrite and NO in TE-15 and OE-19 cell lines, along with mouse serum and tumor tissues, were evaluated using enzyme-linked immunosorbent assay (Figure 8). When NOS1 was overexpressed, nitrite levels increased, while NO levels decreased compared to the control samples. Conversely, when NOS1 was overexpressed and NOS1AP was downregulated, NO levels increased while nitrite levels decreased. To analyze the levels of the cellular adhesion protein E-cadherin and components of the PI3K/AKT signaling pathway, WB was performed (Figure 8). In TE-15 and OE-19 cell lines, oe-NOS1 alone resulted in elevated levels of E-cadherin, p-PI3K/PI3K, and p-AKT/AKT compared to the control group. Conversely, in these same cell lines, co-oe-NOS1 and reduced expression of NOS1AP led to a decrease in E-cadherin, p-PI3K/PI3K, and p-AKT/AKT levels, relative to the situation where only NOS1 was overexpressed.

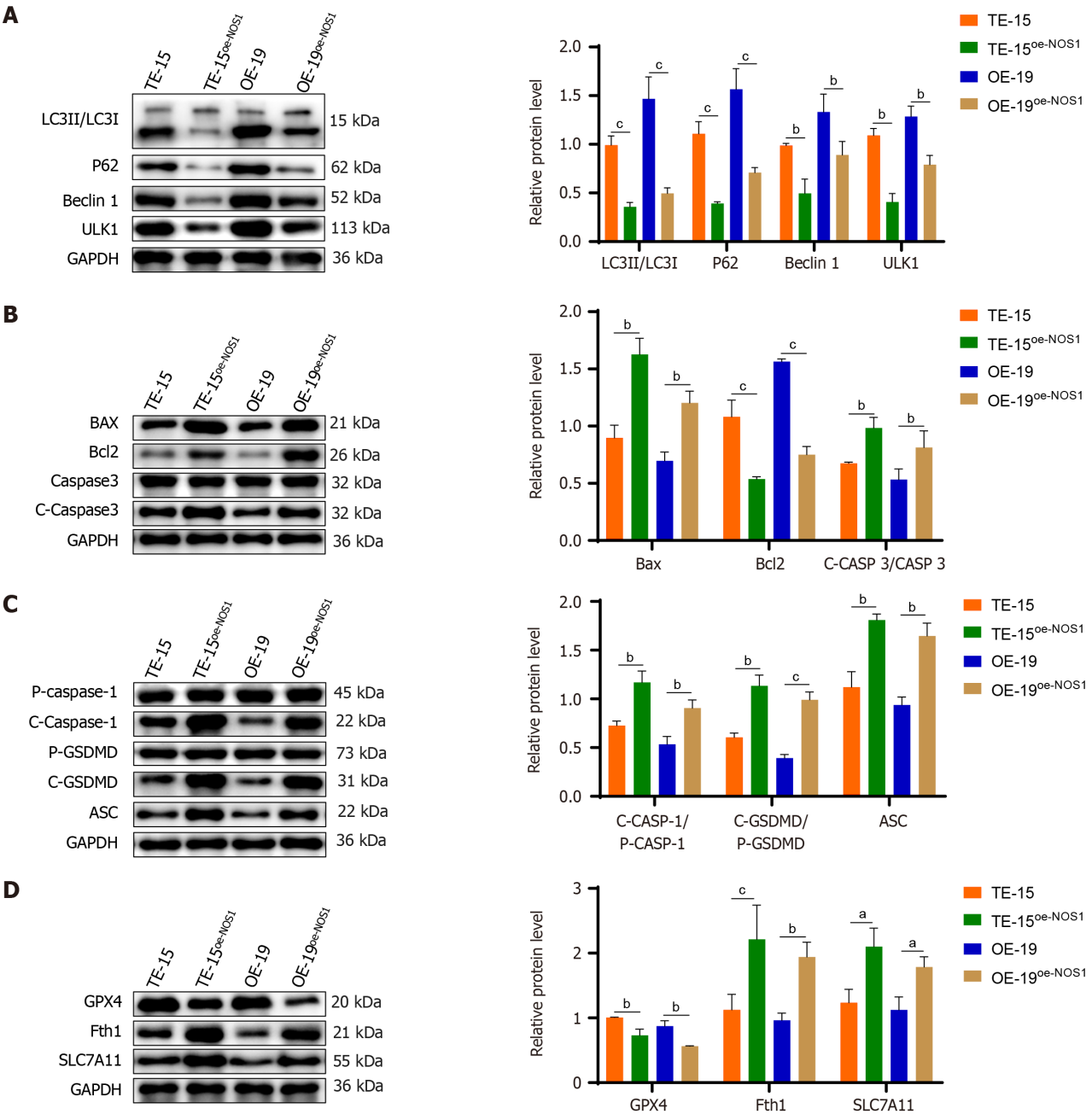

Figure 4 Western blotting to detect the effect of nitric oxide synthase 1 on the levels of autophagy, apoptosis, pyroptosis, and ferroptosis in esophageal cancer cells. A: Autophagy; B: Apoptosis; C: Pyroptosis; D: Ferroptosis. Values are mean ± SD. $^{a}P < 0.05$. $^{b}P < 0.01$. $^{c}P < 0.001$. $n = 3$ experiments. GAPDH: Glyceraldehyde-3-phosphate dehydrogenase; NOS1: Nitric oxide synthase 1; oe-NOS1: Overexpression of nitric oxide synthase 1.

DISCUSSION

NOS1 has been associated with the promotion of tumor development and spread in a range of cancerous lesions[22-24]. Zou *et al*[24] indicated that elevated NOS1 Levels could promote proliferation and invasion in ovarian cancer cells while simultaneously decreasing their responsiveness to chemotherapy. Likewise, Xu *et al*[25] reported that NOS1 aids in the lung metastasis of melanoma *via* epigenetic changes. Ding *et al*[26] discovered that inhibiting NOS1 expression significantly reduced cell proliferation and increased apoptosis in cervical cancer cells. However, the exact function of NOS1 in ESCA is yet to be fully understood. Our research revealed that NOS1 expression in human ESCA cells was considerably lower compared to that in normal human esophageal epithelial cells, which corresponds with findings from raw letter analysis. Further studies demonstrated that oe-NOS1 led to a significant reduction in the functional ability of ESCA cells and tumor growth in murine models. Specifically, tumor cells exhibited a blockade in the G2 phase of interphase during cellular division, potentially protecting them from DNA damage caused by treatments. Importantly, the duration of the G2 phase was reduced with NOS1 overexpression, reinforcing existing literature that suggests an oncogenic role for NOS1 in ESCA[27,28].

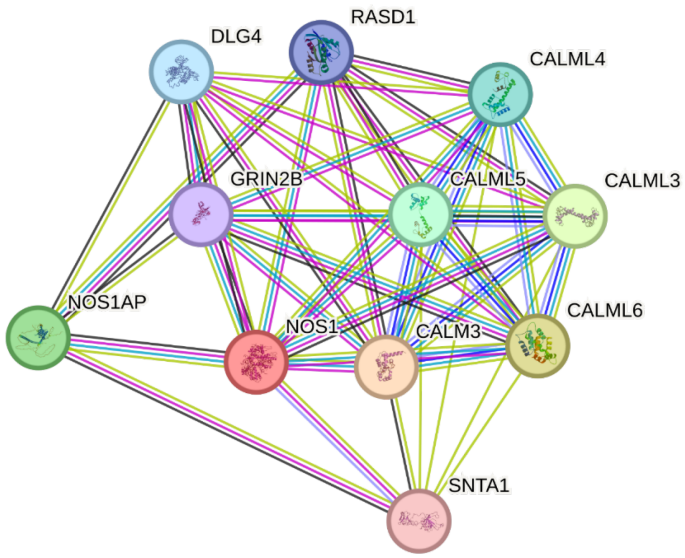

Figure 5 Construction of nitric oxide synthase 1-mediated producer price index network in esophageal cancer. CALM3: Calmodulin 3; CALML3: Calmodulin-like 3; CALML4: Calmodulin-like 4; CALML5: Calmodulin-like 5; CALML6: Calmodulin-like 6; DLG4: Discs large MAGUK scaffold protein 4; GRIN2B: Glutamate receptor, ionotropic, N-methyl D-aspartate 2B; NOS1: Nitric oxide synthase 1; NOS1AP: Nitric oxide synthase 1 adaptor protein; RASD1: Ras-related dexamethasone-induced 1; SNTA1: Syntrophin alpha-1.

Research has shown that processes such as cell autophagy, apoptosis, pyroptosis, and ferroptosis play a crucial role in the viability of ESCA cells. Apoptosis is a key mechanism to prevent tumorigenesis, yet tumor cells typically display suppressed apoptosis levels[29]. Pyroptosis can have a dual influence on tumor progression, either aiding in growth or triggering regression, depending on the surrounding cellular conditions[30]. Ferroptosis, which is defined as a type of cell death that relies on iron and occurs owing to excessive lipid peroxidation, leading to rupture of the plasma membrane, involves both the accumulation of iron and lipid peroxidation, which together induce oxidative damage to membranes [31]. Autophagy is a cellular process that involves the degradation of components to maintain homeostasis and manage lipid metabolism. It facilitates the removal of misfolded or aggregated proteins, the elimination of damaged organelles like mitochondria and the endoplasmic reticulum, and the clearance of intracellular pathogens[32]. Although autophagy is usually considered a survival strategy, it can also enable tumorigenesis and metastasis through various mechanisms during tumor development[33]. Our study specifically examined the impact of NOS1 overexpression on autophagy levels in ESCA cells. Previous studies have indicated that NOS1 acts as a negative regulator of autophagy. After oe-NOS1, autophagy levels diminished, which corresponded with a reduction in cellular function[34].

Analysis of the NOS1 protein interaction network identified multiple proteins that are closely associated with cellular autophagy. A correlation analysis revealed that NOS1AP exhibited the strongest correlation with NOS1. Prior research has demonstrated that polymorphisms in NOS1AP lead to a decrease in NOS1 activity and are connected to prolonged repolarization in arrhythmogenesis[35]. Furthermore, both NOS1 and NOS1AP have been related to the severity of post-traumatic stress disorder, anxiety, stress, depression, and resilience[36]. These results highlight a potential interaction between NOS1 and NOS1AP. However, the roles of NOS1AP and NOS1 in cancer remain somewhat underexplored. Our study corroborates the interactive dynamics between NOS1 and NOS1AP, emphasizing a rise in NOS1AP levels alongside NOS1 levels. We also found that both NOS1 and NOS1AP participate in autophagy in ESCA cells, with their expression affected when autophagy is suppressed. NOS1 expression increased when it was overexpressed alone or when autophagy was inhibited together with NOS1AP inhibition. In contrast, the simultaneous disruption of NOS1AP and autophagy led to elevated NOS1 expression, diminished proliferative capabilities, and heightened apoptosis in ESCA cells. These findings highlight a significant relationship between NOS1, NOS1AP, and autophagy regulation in ESCA.

NO serves as a crucial regulatory element in autophagy, and any irregularities or dysfunctions in the NO signaling pathway can trigger tumor development and progression. NO affects cell cycle dynamics and apoptosis, playing a pivotal role in cellular growth and tumor advancement. Anomalous expression of NO may result in excessive proliferation of tumor cells and promote tumorigenesis[37]. Tumor tissues can accumulate nitrite, which aids in the breakdown of the extracellular matrix and supports the invasion and spread of malignant cells[38]. In addition, nitrite fosters angiogenesis in malignant tumors. Research indicates that nitrite can enhance the migration and invasion of hepatocellular carcinoma cells *via* mitochondrial autophagy[39]. Our investigation proposes that variations in NO and nitrite levels, associated with changes in the expression of NOS1 and NOS1AP, suggest that these enzymes work together to regulate both NO and nitrite concentrations, influencing cellular autophagy. Moreover, activation of the PI3K/AKT signaling pathway appears to inhibit cellular autophagy. While our findings indicate that stimulation of the PI3K/AKT pathway by NOS1 and NOS1AP leads to reduced autophagy, it has yet to be established whether this pathway is responsible for mediating the regulatory effects of NOS1 and NOS1AP on NO and nitrite levels, thereby reducing autophagy. Previous studies point out that levels of NO and nitrite also vary following the inhibition of the PI3K/AKT pathway; therefore, we postulate that NOS1 and NOS1AP may influence NO and nitrite concentrations through this pathway, ultimately affecting cellular autophagy.

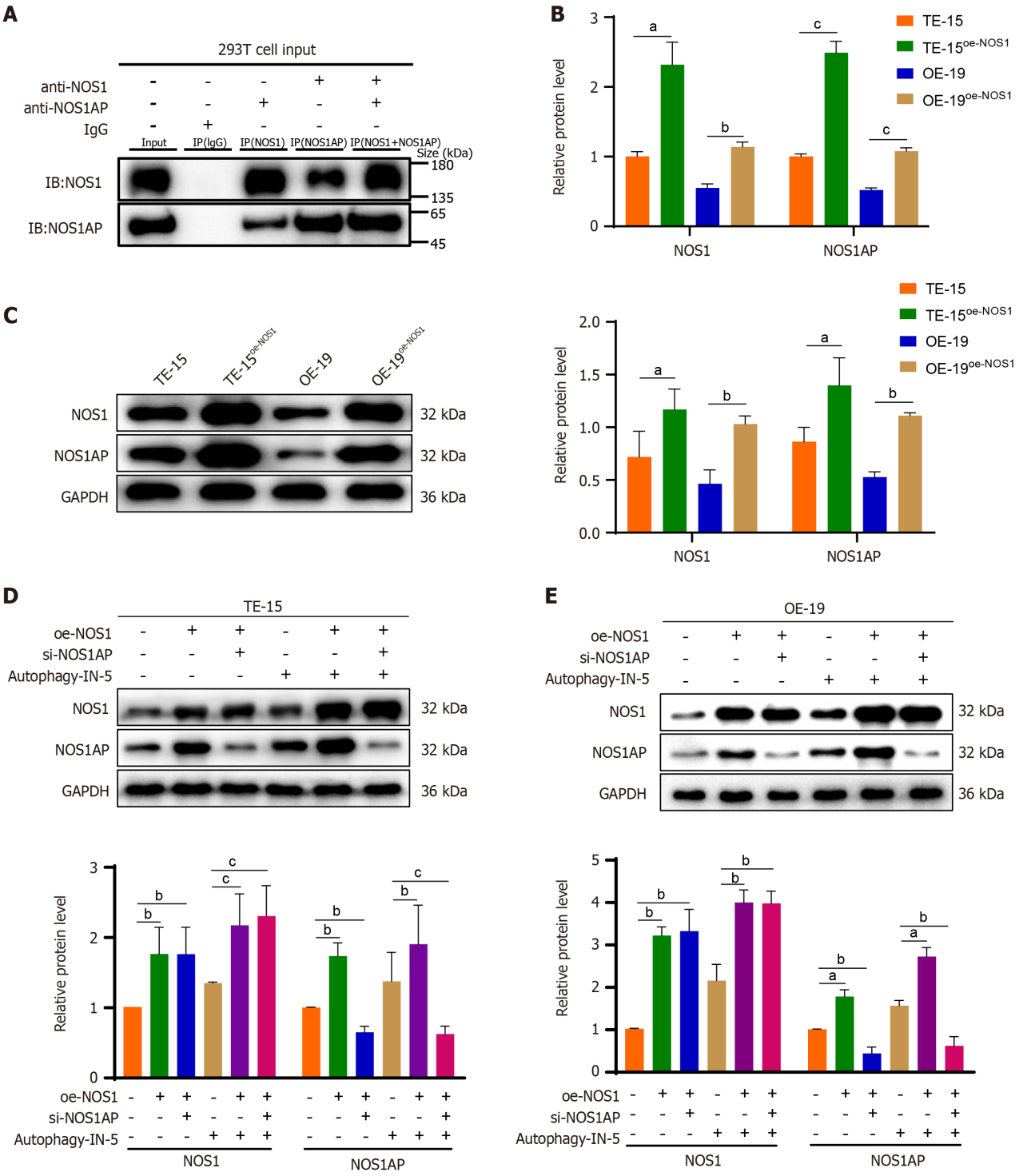

Figure 6 Nitric oxide synthase 1 and nitric oxide synthase 1 adaptor protein interaction. A: Immunoprecipitation analysis of the interaction between nitric oxide synthase 1 (NOS1) and nitric oxide synthase 1 adaptor protein (NOS1AP); B and C: Effect of NOS1 expression level on NOS1AP expression level; Quantitative real-time polymerase chain reaction (B); Western blotting (C); D and E: Western Blotting to detect the changes of NOS1 and NOS1AP expression in TE-15 and OE-19 cell lines after inhibition of autophagy; TE-15 cell line (D); OE-19 cell line (E). Values are mean ± SD. $^{a}P < 0.05$. $^{b}P < 0.01$. $^{c}P < 0.001$. $n = 3$ experiments. NOS1: Nitric oxide synthase 1; NOS1AP: Nitric oxide synthase 1 adaptor protein; IB: Immunoblotting; IP: Immunoprecipitation; oe-NOS1: Overexpression of nitric oxide synthase 1; GAPDH: Glyceraldehyde-3-phosphate dehydrogenase; si-NOS1AP: Silencing of nitric oxide synthase 1 adaptor protein.

CONCLUSION

Our study demonstrated that the co-expression of NOS1 and NOS1AP affected autophagy levels and regulated the PI3K/AKT signaling pathway. In summary, our findings suggest that NOS1 and NOS1AP may regulate autophagy in ESCA cells by modulating the PI3K/AKT pathway.

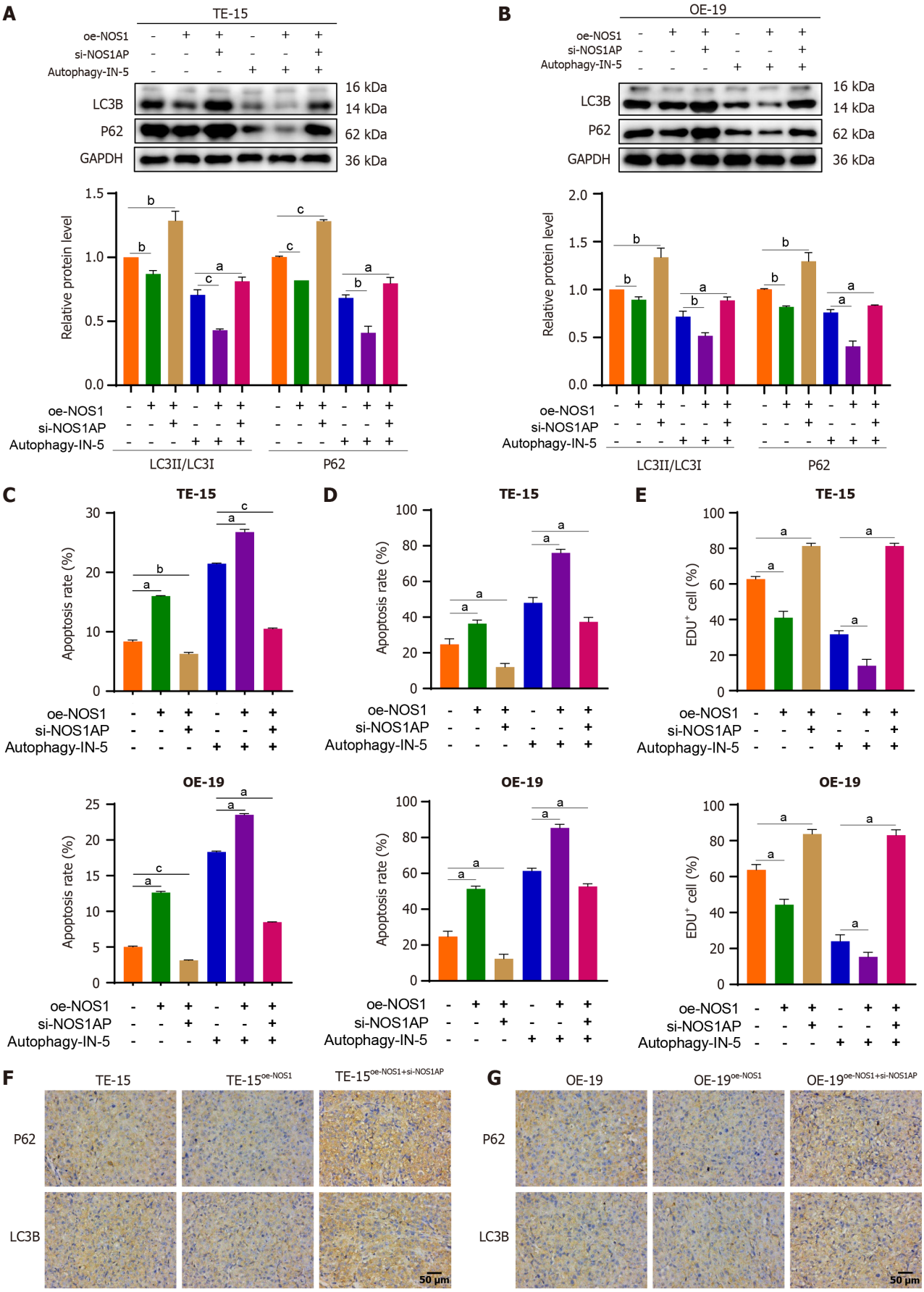

Figure 7 Nitric oxide synthase 1 and nitric oxide synthase 1 adaptor protein affect the level of cell autophagy and apoptosis. A and B: Western blotting detected the changes in the expression of autophagy-related proteins LC3B and P62 in TE-15 and OE-19 cell lines; C: Flow cytometry analyzed the level of apoptosis; D: TUNEL staining analyzed the level of apoptosis; E: 5-Ethynyl-2'-deoxyuridine assay analyzed the cell proliferation ability; F and G:

Immunohistochemistry analysis of P62, LC3B expression in mouse tumor tissues. Values are mean ± SD. [a]*P* < 0.05. [b]*P* < 0.01. [c]*P* < 0.001. *n* = 3 experiments. EDU: 5-Ethynyl-2'-deoxyuridine; oe-NOS1: Overexpression of nitric oxide synthase 1; GAPDH: Glyceraldehyde-3-phosphate dehydrogenase; si-NOS1AP: Silencing of nitric oxide synthase 1 adaptor protein.

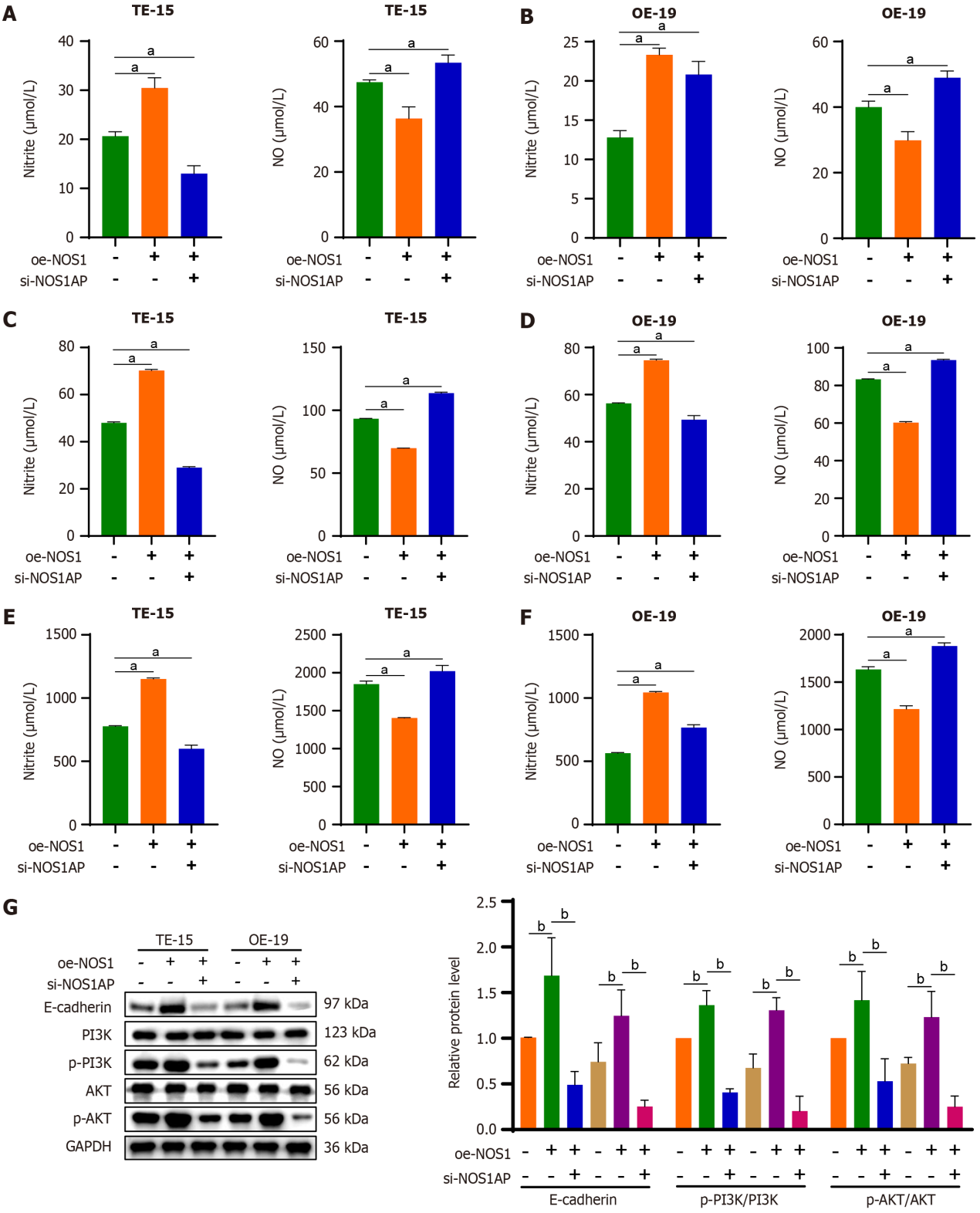

Figure 8 Effect of nitric oxide synthase 1 and nitric oxide synthase 1 adaptor protein on the expression of nitric oxide, nitrite, and phosphatidylinositol 3-kinase/protein kinase B pathway-related proteins. Enzyme-linked immunosorbent assay to detect nitric oxide and nitrite in different samples. A: TE-15 cell line; B: OE-19 cell line; C and D: Mouse serum; E and F: Tumor tissues; G: Western Blotting was performed to detect the expression of phosphatidylinositol 3-kinase (PI3K)/protein kinase B (AKT) pathway-related proteins E-cadherin, phosphorylated (p)-PI3K/PI3K, p-AKT/AKT. Values are mean ±

SD. [a]*P* < 0.05. [b]*P* < 0.01. [c]*P* < 0.001. *n* = 3 experiments. oe-NOS1: Overexpression of nitric oxide synthase 1; NO: Nitric oxide; si-NOS1AP: Silencing of nitric oxide synthase 1 adaptor protein; PI3K: Phosphatidylinositol 3-kinase; AKT: Protein kinase B.

FOOTNOTES

Author contributions: Li L and Xiao ZW designed the experiments, wrote the manuscript, and revised it; Zeng YC, Ji LT, and Yuan JT performed the experiments. All authors contributed to the analysis of the results and approved the final manuscript.

Supported by the National Natural Science Foundation of China, No. 81000201.

Institutional review board statement: This study does not involve any human experiments.

Institutional animal care and use committee statement: All animal experiments were approved by the Animal Ethical and Welfare Committee of Guangzhou Miles Biosciences, (No. MIS20230070).

Conflict-of-interest statement: The authors declare that they have no conflict of interest.

Data sharing statement: The datasets used and/or analyzed during the current study are available from the corresponding author upon reasonable request.

ARRIVE guidelines statement: The authors have read the ARRIVE guidelines, and the manuscript was prepared and revised according to the ARRIVE guidelines.

Country of origin: China

ORCID number: Lin Li 0009-0002-7763-4733.

S-Editor: Fan M
L-Editor: Filipodia
P-Editor: Guo X

REFERENCES

1 **Alsop BR**, Sharma P. Esophageal Cancer. *Gastroenterol Clin North Am* 2016; **45**: 399-412 [PMID: 27546839 DOI: 10.1016/j.gtc.2016.04.001]
2 **Nienhüser H**, Wirsik N, Schmidt T. Esophageal Tumor Microenvironment. *Adv Exp Med Biol* 2020; **1296**: 103-116 [PMID: 34185288 DOI: 10.1007/978-3-030-59038-3_6]
3 **Wen J**, Xuan B, Liu Y, Wang L, He L, Meng X, Zhou T, Wang Y. NLRP3 inflammasome-induced pyroptosis in digestive system tumors. *Front Immunol* 2023; **14**: 1074606 [PMID: 37081882 DOI: 10.3389/fimmu.2023.1074606]
4 **Lohan-Codeço M**, Barambo-Wagner ML, Nasciutti LE, Ribeiro Pinto LF, Meireles Da Costa N, Palumbo A Jr. Molecular mechanisms associated with chemoresistance in esophageal cancer. *Cell Mol Life Sci* 2022; **79**: 116 [PMID: 35113247 DOI: 10.1007/s00018-022-04131-6]
5 **Wang Z**, Wu S, Zhu C, Shen J. The role of ferroptosis in esophageal cancer. *Cancer Cell Int* 2022; **22**: 266 [PMID: 35999642 DOI: 10.1186/s12935-022-02685-w]
6 **Liu K**, Zhao T, Wang J, Chen Y, Zhang R, Lan X, Que J. Etiology, cancer stem cells and potential diagnostic biomarkers for esophageal cancer. *Cancer Lett* 2019; **458**: 21-28 [PMID: 31125642 DOI: 10.1016/j.canlet.2019.05.018]
7 **Li Y**, Yang Q, Chen H, Yang X, Han J, Yao X, Wei X, Si J, Yao H, Liu H, Wan L, Yang H, Wang Y, Bao D. TFAM downregulation promotes autophagy and ESCC survival through mtDNA stress-mediated STING pathway. *Oncogene* 2022; **41**: 3735-3746 [PMID: 35750756 DOI: 10.1038/s41388-022-02365-z]
8 **Yang W**, Cheng B, Chen P, Sun X, Wen Z, Cheng Y. BTN3A1 promotes tumor progression and radiation resistance in esophageal squamous cell carcinoma by regulating ULK1-mediated autophagy. *Cell Death Dis* 2022; **13**: 984 [PMID: 36418890 DOI: 10.1038/s41419-022-05429-w]
9 **Li M**, Li X, Chen S, Zhang T, Song L, Pei J, Sun G, Guo L. IPO5 Mediates EMT and Promotes Esophageal Cancer Development through the RAS-ERK Pathway. *Oxid Med Cell Longev* 2022; **2022**: 6570879 [PMID: 36120598 DOI: 10.1155/2022/6570879]
10 **Fang F**, Li Y, Chang L. Mechanism of autophagy regulating chemoresistance in esophageal cancer cells. *Exp Mol Pathol* 2020; **117**: 104564 [PMID: 33137292 DOI: 10.1016/j.yexmp.2020.104564]
11 **Glick D**, Barth S, Macleod KF. Autophagy: cellular and molecular mechanisms. *J Pathol* 2010; **221**: 3-12 [PMID: 20225336 DOI: 10.1002/path.2697]
12 **Liu S**, Yao S, Yang H, Liu S, Wang Y. Autophagy: Regulator of cell death. *Cell Death Dis* 2023; **14**: 648 [PMID: 37794028 DOI: 10.1038/s41419-023-06154-8]
13 **Debnath J**, Gammoh N, Ryan KM. Autophagy and autophagy-related pathways in cancer. *Nat Rev Mol Cell Biol* 2023; **24**: 560-575 [PMID: 36864290 DOI: 10.1038/s41580-023-00585-z]

14 **Li X**, He S, Ma B. Autophagy and autophagy-related proteins in cancer. *Mol Cancer* 2020; **19**: 12 [PMID: 31969156 DOI: 10.1186/s12943-020-1138-4]

15 **Poillet-Perez L**, White E. Role of tumor and host autophagy in cancer metabolism. *Genes Dev* 2019; **33**: 610-619 [PMID: 31160394 DOI: 10.1101/gad.325514.119]

16 **Krylatov A**, Maslov L, Tsibulnikov SY, Voronkov N, Boshchenko A, Downey J, Mentzer R. The Role of Reactive Oxygen Species, Kinases, Hydrogen Sulfide, and Nitric Oxide in the Regulation of Autophagy and Their Impact on Ischemia and Reperfusion Injury in the Heart. *Curr Cardiol Rev* 2021; **17**: e230421186874 [PMID: 33059566 DOI: 10.2174/1573403X16666201014142446]

17 **Zhang X**, Jin L, Tian Z, Wang J, Yang Y, Liu J, Chen Y, Hu C, Chen T, Zhao Y, He Y. Nitric oxide inhibits autophagy and promotes apoptosis in hepatocellular carcinoma. *Cancer Sci* 2019; **110**: 1054-1063 [PMID: 30657629 DOI: 10.1111/cas.13945]

18 **He Q**, Qu M, Xu C, Shi W, Hussain M, Jin G, Zhu H, Zeng LH, Wu X. The emerging roles of nitric oxide in ferroptosis and pyroptosis of tumor cells. *Life Sci* 2022; **290**: 120257 [PMID: 34952041 DOI: 10.1016/j.lfs.2021.120257]

19 **Tran AN**, Boyd NH, Walker K, Hjelmeland AB. NOS Expression and NO Function in Glioma and Implications for Patient Therapies. *Antioxid Redox Signal* 2017; **26**: 986-999 [PMID: 27411305 DOI: 10.1089/ars.2016.6820]

20 **Kanwar JR**, Kanwar RK, Burrow H, Baratchi S. Recent advances on the roles of NO in cancer and chronic inflammatory disorders. *Curr Med Chem* 2009; **16**: 2373-2394 [PMID: 19601787 DOI: 10.2174/092986709788682155]

21 **Wang J**, Jin L, Zhu Y, Zhou X, Yu R, Gao S. Research progress in NOS1AP in neurological and psychiatric diseases. *Brain Res Bull* 2016; **125**: 99-105 [PMID: 27237129 DOI: 10.1016/j.brainresbull.2016.05.014]

22 **Chen X**, Zou Z, Wang Q, Gao W, Zeng S, Ye S, Xu P, Huang M, Li K, Chen J, Zhong Z, Zhang Q, Hao B, Liu Q. Inhibition of NOS1 promotes the interferon response of melanoma cells. *J Transl Med* 2022; **20**: 205 [PMID: 35538490 DOI: 10.1186/s12967-022-03403-w]

23 **Wang Q**, Ye S, Chen X, Xu P, Li K, Zeng S, Huang M, Gao W, Chen J, Zhang Q, Zhong Z, Liu Q. Mitochondrial NOS1 suppresses apoptosis in colon cancer cells through increasing SIRT3 activity. *Biochem Biophys Res Commun* 2019; **515**: 517-523 [PMID: 31153640 DOI: 10.1016/j.bbrc.2019.05.114]

24 **Zou Z**, Li X, Sun Y, Li L, Zhang Q, Zhu L, Zhong Z, Wang M, Wang Q, Liu Z, Wang Y, Ping Y, Yao K, Hao B, Liu Q. NOS1 expression promotes proliferation and invasion and enhances chemoresistance in ovarian cancer. *Oncol Lett* 2020; **19**: 2989-2995 [PMID: 32218855 DOI: 10.3892/ol.2020.11355]

25 **Xu P**, Ye S, Li K, Huang M, Wang Q, Zeng S, Chen X, Gao W, Chen J, Zhang Q, Zhong Z, Lin Y, Rong Z, Xu Y, Hao B, Peng A, Ouyang M, Liu Q. NOS1 inhibits the interferon response of cancer cells by S-nitrosylation of HDAC2. *J Exp Clin Cancer Res* 2019; **38**: 483 [PMID: 31805977 DOI: 10.1186/s13046-019-1448-9]

26 **Ding M**, Zhang H, Liu L, Liang R. Effect of NOS1 regulating ABCG2 expression on proliferation and apoptosis of cervical cancer cells. *Oncol Lett* 2019; **17**: 1531-1536 [PMID: 30675209 DOI: 10.3892/ol.2018.9786]

27 **Ramedani F**, Jafari SM, Saghaeian Jazi M, Mohammadi Z, Asadi J. Anti-cancer effect of entacaponeon esophageal cancer cells *via* apoptosis induction and cell cycle modulation. *Cancer Rep (Hoboken)* 2023; **6**: e1759 [PMID: 36534072 DOI: 10.1002/cnr2.1759]

28 **Chen Z**, Tang W, Ye W, Song L, Chen Z. ADAMTS9-AS2 regulates PPP1R12B by adsorbing miR-196b-5p and affects cell cycle-related signaling pathways inhibiting the malignant process of esophageal cancer. *Cell Cycle* 2022; **21**: 1710-1725 [PMID: 35503407 DOI: 10.1080/15384101.2022.2067675]

29 **Wong RS**. Apoptosis in cancer: from pathogenesis to treatment. *J Exp Clin Cancer Res* 2011; **30**: 87 [PMID: 21943236 DOI: 10.1186/1756-9966-30-87]

30 **Rao Z**, Zhu Y, Yang P, Chen Z, Xia Y, Qiao C, Liu W, Deng H, Li J, Ning P, Wang Z. Pyroptosis in inflammatory diseases and cancer. *Theranostics* 2022; **12**: 4310-4329 [PMID: 35673561 DOI: 10.7150/thno.71086]

31 **Hassannia B**, Vandenabeele P, Vanden Berghe T. Targeting Ferroptosis to Iron Out Cancer. *Cancer Cell* 2019; **35**: 830-849 [PMID: 31105042 DOI: 10.1016/j.ccell.2019.04.002]

32 **Saxena R**, Klochkova A, Murray MG, Kabir MF, Samad S, Beccari T, Gang J, Patel K, Hamilton KE, Whelan KA. Roles for Autophagy in Esophageal Carcinogenesis: Implications for Improving Patient Outcomes. *Cancers (Basel)* 2019; **11** [PMID: 31683722 DOI: 10.3390/cancers11111697]

33 **Ferro F**, Servais S, Besson P, Roger S, Dumas JF, Brisson L. Autophagy and mitophagy in cancer metabolic remodelling. *Semin Cell Dev Biol* 2020; **98**: 129-138 [PMID: 31154012 DOI: 10.1016/j.semcdb.2019.05.029]

34 **Zhou W**, Yao Y, Li J, Wu D, Zhao M, Yan Z, Pang A, Kong L. TIGAR Attenuates High Glucose-Induced Neuronal Apoptosis *via* an Autophagy Pathway. *Front Mol Neurosci* 2019; **12**: 193 [PMID: 31456661 DOI: 10.3389/fnmol.2019.00193]

35 **Ronchi C**, Bernardi J, Mura M, Stefanello M, Badone B, Rocchetti M, Crotti L, Brink P, Schwartz PJ, Gnecchi M, Zaza A. NOS1AP polymorphisms reduce NOS1 activity and interact with prolonged repolarization in arrhythmogenesis. *Cardiovasc Res* 2021; **117**: 472-483 [PMID: 32061134 DOI: 10.1093/cvr/cvaa036]

36 **Bruenig D**, Morris CP, Mehta D, Harvey W, Lawford B, Young RM, Voisey J. Nitric oxide pathway genes (NOS1AP and NOS1) are involved in PTSD severity, depression, anxiety, stress and resilience. *Gene* 2017; **625**: 42-48 [PMID: 28465168 DOI: 10.1016/j.gene.2017.04.048]

37 **Hu Y**, Xiang J, Su L, Tang X. The regulation of nitric oxide in tumor progression and therapy. *J Int Med Res* 2020; **48**: 300060520905985 [PMID: 32090657 DOI: 10.1177/0300060520905985]

38 **Panneerselvan P**, Vasanthakumar K, Muthuswamy K, Krishnan V, Subramaniam S. Insights on the functional dualism of nitric oxide in the hallmarks of cancer. *Biochim Biophys Acta Rev Cancer* 2023; **1878**: 189001 [PMID: 37858621 DOI: 10.1016/j.bbcan.2023.189001]

39 **Maekawa H**, Iwabuchi K, Nagaoka I, Watanabe H, Kamano T, Tsurumaru M. Activated peritoneal macrophages inhibit the proliferation of rat ascites hepatoma AH-130 cells *via* the production of tumor necrosis factor-alpha and nitric oxide. *Inflamm Res* 2000; **49**: 541-547 [PMID: 11089907 DOI: 10.1007/s000110050629]

Published by **Baishideng Publishing Group Inc**
7041 Koll Center Parkway, Suite 160, Pleasanton, CA 94566, USA
Telephone: +1-925-3991568
E-mail: office@baishideng.com
Help Desk: https://www.f6publishing.com/helpdesk
https://www.wjgnet.com